ACS OMEGA

Open Access

http://pubs.acs.org/journal/acsodf

Article

Silver Nanowire-Coated Porous Alginate Films for Wound Dressing Applications: Antibacterial Activity, Cell Proliferation, and Physical Characterization

Nilay Kahya, Aslin Kartun, Işık Neslişah Korkut, Canan Usta, Dürdane Serap Kuruca, and Alper Gürarslan*

Cite This: *ACS Omega* 2024, 9, 49032−49042

Read Online

ACCESS | Metrics & More | Article Recommendations | Supporting Information

ABSTRACT: In the present study, porous calcium alginate films have been developed by the addition of 0.02, 0.1, and 0.5% (w/v) PVA to sodium alginate film solutionss. Poly(vinyl) alcohol played the role of a pore-forming agent for calcium alginate films, and the controlled pore sizes of the films were investigated by scanning electron microscopy and Fourier transform infrared spectroscopy analyses. Human fibroblast cell attachment was performed on the porous calcium alginate films (0.5-Ca-Alg), and then the film was coated with 1 and 3 wt % silver nanowires. Cell proliferation was enhanced on films after the coating of the silver nanowires. The MTT assay was performed on the calcium alginate films and silver nanowire-coated films, and the films were found to be nontoxic to human foreskin fibroblast cells at the end of 72 h of exposure. The existence of silver nanowires on the porous calcium alginate film endowed the material with good antibacterial activity. The swelling ability of the porous and silver nanowire-coated film (0.5-Ca-Alg-1/AgNW) increased by ∼64% in simulated body fluid (pH = 7.4) and distilled water compared to a nonporous film (Ca-Alg). The water vapor transmission rate of Ca-Alg was ∼45% enhanced thanks to the porosity of films and the existence of AgNW. Hereby, it is demonstrated that the novel silver nanowire-doped porous alginate materials would be potential wound dressing agents with desired physical properties, antibacterial activity, and availability to cell proliferation.

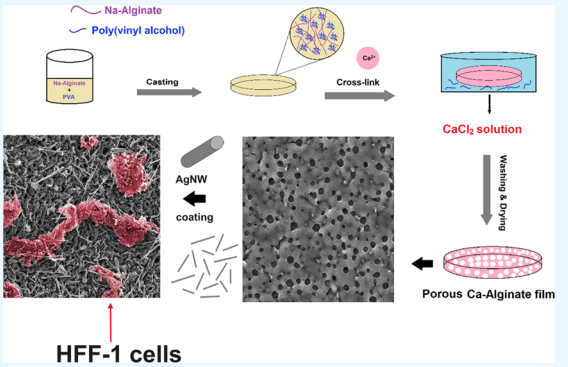

1. INTRODUCTION

All over the world, scientists continue to develop healthcare products that are environmentally friendly and beneficial to patients using smart technologies.[1,2] One such type of product that is needed for practical treatments is wound dressing or wound care materials in the medical field. Various types of wound healing products have been developed through the centuries for wounds to protect them from external factors, contributing to their healing process. Recently, traditional wound dressings such as gauze, bandages, or cotton have been mainly replaced by modern wound dressings, which are designed as hydrocolloids, foams, hydrogels, and films with advantageous properties.[3−5] Wound dressings should possess certain characteristic features to be commercialized and to gain widespread applications. For example, nontoxicity, biodegradability, biocompatibility, good mechanical properties, protection of the wound from infections, and ability to absorb moisture are common desired properties of various wound care products.[6−8] Additionally, being antibacterial along with these properties will endow wound care products with a great advantage in the wound healing process. The antibacterial properties of dressings can be improved by impregnating an antibacterial agent.[9−11]

Silver has been utilized in medicine for healthcare purposes, one of which is acquiring antimicrobial conditions.[12−14] In order to incorporate silver into wound dressing materials, silver compounds can be added as silver salts or silver nanoparticles in various sizes.[15,16] The silver-incorporated wound dressing materials have been clinically treated for wound care studies.[17−19] Silver nanoparticles with their attractive antibacterial properties have been formulated in wound dressing applications.[20−23] Silver nanoparticle-added polymer-type wound dressings are already interesting owing to their good antibacterial activities.[24,25] Baukum et al. prepared a wound dressing candidate, a silver nanoparticle-doped calcium chloride cross-linked alginate/gelatin hydrogel, which is antibacterial against *Escherichia coli*, *Pseudomonas aeruginosa*, and *Staphylococcus aureus* bacteria. Cell culture studies of the

Received: March 13, 2024
Revised: September 26, 2024
Accepted: October 2, 2024
Published: December 5, 2024

hydrogel were performed, and it was found that the hydrogel containing silver nanoparticles was nontoxic to both the human dermal fibroblast cell line (NHDF) and NCTC clone 929 cells.[24] Diniz et al. developed silver nanoparticle-containing alginate−gelatin hydrogels, which showed antimicrobial activity against *S. aureus* and *P. aeruginosa* bacteria and noncytotoxicity to human fibroblast L929 cell lines. It was observed that the existence of the nanoparticles helped speed up the formation of tissues, which provided faster healing for collagen scars.[25]

Silver nanowires (AgNWs) among silver nanospecies have gained great research interest recently. AgNWs have been subjected to various discipline applications: wearable electronics, biomedical devices, solar cells, biosensors, etc.[26−30] To benefit from the antibacterial activity of AgNWs,[31] AgNWs can be employed as a remarkable silver doping agent in the preparation of composite wound dressings. Li et al. produced AgNW-thiolated chitosan scaffold hydrogel films with gained antibacterial activity against *E. coli* and *S. aureus* by silver nanowire incorporation. The existence of AgNWs in the chitosan film supported significant wound healing of the skin wounds of rabbits.[32] Wan et al. investigated biocompatible AgNW-bacterial cellulose dressings, which are antibacterial against *S. aureus* and *E. coli*, and found that the incorporation of silver nanowires into bacterial cellulose made the healing of the wound site quick and completely healed the wound of the test animal.[33] A recent study has shown that silver nanowire/polylactic acid nanofiber membranes containing 5 wt % AgNWs show good antimicrobial activity and cell adhesion of mouse fibroblasts (L929) on the membranes.[34]

Alginate (Alg) is a polysaccharide structure biopolymer and has gained acceptance in the form of a wound dressing on its own or in combination with other natural or synthetic polymers.[24,25,35] In fact, many commercialized alginate dressings have taken their place in the market and are already being used.[36−39] In special cases, permeability in wound dressings is a desired feature for wound care.[40,41] It is important for flat-surfaced calcium alginate films[42] as a wound dressing candidate to gain porosity that will increase the permeability and at the same time increase the cell proliferation in the area, where they are in contact with the wound.

In this study, a strategy was first developed for the films, which were cast with Na-Alg/PVA content and cross-linked by calcium chloride in order to gain a porous structure. First, to prepare porous Ca-Alg films, sodium alginate (Na-Alg) was mixed with an aqueous poly(vinyl) alcohol (PVA) solution in this study. Then, varied amounts of PVA-doped Na-Alg films were cross-linked by calcium chloride solutions. For the characterization of the films, scanning electron microscopy and Fourier transform infrared spectroscopy analyses were performed. The dissolution of PVA from the films was achieved while curing the films in aqueous solutions during the cross-linking and washing stages. As far as our knowledge of AgNW−biopolymer composites in the literature, there has not yet been any study of coating AgNWs onto calcium alginate films for wound healing applications. To be a wound dressing candidate, porous Ca-Alg films were coated with AgNWs, and cell proliferation studies were attempted. Antibacterial properties against both Gram-positive (*S. aureus*) and Gram-negative (*E. coli*) bacteria and cell adhesion ability on AgNW-coated porous Ca-Alg films were investigated. In the investigation step of the physical properties of films, the light transmittance properties of porous AgNW-coated Ca-Alg films were determined, their water vapor permeability was examined, and the water uptake behavior of the films in water or simulated body fluid was monitored.

2. EXPERIMENTAL SECTION

2.1. Materials. Sodium alginate (Catalog number: W201502, 1% aqueous solution with a viscosity of 5.0 at 25 °C), poly(vinyl alcohol) (average molecular weight (M_w) of 130 000 g mol^{-1}; 99+ % hydrolyzed), and 3-(4,5-dimethyl-2-thiazolyl)-2,5-diphenyl-2H-tetrazolium bromide (MTT) were purchased from Sigma-Aldrich (St. Louis, Missouri). Sodium chloride, sodium bicarbonate, potassium chloride, potassium dihydrogen phosphate, magnesium chloride hexahydrate, hydrochloric acid (fuming 37% for analysis), calcium chloride dihydrate, sodium sulfate, tris(hydroxymethyl)aminomethane (Tris), and ethanol (absolute for analysis) were from Merck (Darmstadt, Germany). All chemicals were analytical grade and were used without any further purification. All solutions were prepared with distilled water produced by a Nüve NS 103 (Ankara, Turkey) water distiller.

2.2. Preparation of Alginate-Based Films. PVA is a synthetic polymer, has nontoxicity and biodegradability, and has been formulated in a lot of different wound dressing designs to improve the material's physical characteristics.[43] The potential of Alg/PVA films as wound dressings is going to be the subject of many new studies.[35] To prepare porous alginate films, a certain weighed amount of PVA was dissolved in hot distilled water while heating the solution at about 80 °C with constant stirring for 1 h using a magnetic stirrer on an IKA C-MAG HS 7 model heater (IKA-Werke GmbH & Co. KG, Staufen, Germany). After the PVA solution was cooled to room temperature, sodium alginate (Na-Alg) powder was added to obtain a 2% (w/v) polymer concentration in the final solution. The Na-Alg/PVA binary mixture was stirred magnetically at room temperature for 3 h for homogenization. Following the complete blending of the polymers, a volume of 10 mL of this polymer solution was poured onto a polystyrene Petri dish, which had a size of 60 mm × 15 mm, and then dried in an oven (Nüve EV 018, Ankara, Turkey) at 40 °C for 24 h. To obtain cross-linked Alg composite films, the dry state of cast films was dipped into 50 mL of 1.5% (w/v) $CaCl_2$ solution for 1 h. Ca^{2+} ion cross-linked films were dipped into a volume of 100 mL of distilled water for 2 h and then rinsed thoroughly with distilled water. Finally, Ca-Alg films were kept for drying at 23 ± 2 °C and 65 ± 5% humidity room conditions for 48 h. The compositions of the formulated Ca-Alg films are listed in Table 1.

2.3. Scanning Electron Microscopy Analysis. Scanning electron microscopy (SEM) images were taken in the secondary electron (SE) mode under vacuum at 15 kV and working distances of 10 mm using a Tescan Vega3 XMU model (TESCAN, Brno, Czech Republic) scanning electron

Table 1. Nomenclature of Porous Ca-Alg Films Cross-Linked in a 1.5% (w/v) $CaCl_2$ Solution

film sample code	Na-Alg, % (w/v)	PVA, % (w/v)
Ca-Alg (control)	2	
0.02-Ca-Alg	2	0.02
0.1-Ca-Alg	2	0.1
0.5-Ca-Alg	2	0.5

https://doi.org/10.1021/acsomega.4c02467
ACS Omega 2024, 9, 49032−49042

microscope. The film samples were coated with Au/Pd by using a Quorum SC7620 Mini Sputter Coater (Quorum Technologies Ltd., Laughton, England) before the scanning operations. The SEM images of film samples were colored by a simple photo editing application, and the original SEM micrographs are given in the Supporting Information.

2.4. FTIR Spectroscopy Analysis. FTIR analysis of the films was performed by a PerkinElmer Spectrum Two FTIR Spectrometer (Shelton, Connecticut). The Ca-Alg-based film samples' transmittance spectra were recorded in the wavelength range from 4000 to 400 cm^{-1}.

2.5. AgNW Coating of Films. To prepare AgNW-coated Ca-Alg films, AgNWs were synthesized according to the method used in our previous studies.[26,27] The freshly prepared AgNW precipitate was dispersed in ethanol under ultrasonification in an ultrasonic bath (ISOLAB Laborgeräte GmbH, Eschau, Germany). Following 15 min sonication of AgNWs in ethanol, the mixture was added by a micropipette on the film sample several times from both film surfaces within 1 min of coating time, which was determined after the preliminary coating experiments. After the film pieces were coated by AgNW−ethanol dispersion, these samples were left to dry on a polystyrene Petri dish for 30 min. Then, the coated film samples were weighed immediately after drying, and the increased mass of the film due to the accumulation of AgNWs on the film surface was calculated by the comparison of the initial and final weights of the film sample. It was observed that the Ca-Alg film with a nonporous surface was coated homogeneously with AgNWs. The AgNW weight content of the final samples was fixed as 1 or 3% for the weight of AgNWs per gram of the dry film in this study. The 1 and 3 wt % AgNW-coated porous calcium alginate films of this study were named 0.5-Ca-Alg-1/AgNW and 0.5-Ca-Alg-3/AgNW, respectively. AgNW-coated Ca-Alg film samples were covered with aluminum foil and kept in the dark under laboratory conditions before their cell culture and cell adhesion analysis.

Figure S1 shows the SEM image of the synthesized AgNWs of this study that have a length between 2 and 5 μm. Hu et al., similarly, performed the coating of bacterial cellulose films by AgNWs, which had an average length of 2−3 μm.[44]

2.6. Cell Adhesion Assay. Human foreskin fibroblast (HFF-1) cells were cultured in Dulbecco's modified Eagle medium (DMEM, Gibco) with 10% fetal bovine serum (FBS, Gibco) and 1% penicillin/streptomycin in a humidified 5% CO_2 incubator and maintained at 37 °C. When the cells reached 80% confluence, they were trypsinized with 0.25% Trypsin−EDTA for passaging and seeding each time. The confluent cells were used in cell adhesion studies.

As the first step in the protocol, the film samples were sterilized with UV light for 4 h and were placed in 6-well plates. HFF-1 cells (about 6×10^5 cells per well) were seeded over the film samples with 3 mL of DMEM solution and incubated for 5 days. After the incubation, the medium was removed and the films were washed with phosphate buffer solution (PBS). The samples were fixed with a 3% glutaraldehyde solution (about 1 mL each well) for 1 h. Then, the films were washed again with PBS. For the dehydration of the samples, the films were incubated in an increasing concentration of alcohol solution series (30, 50, 70, 80, and 90% v/v) for 10 min per step and 30 min (96% v/v) at the last step. The samples used in the cell adhesion assay were dried for 24 h, and they were analyzed with SEM analysis.

2.7. MTT Cytotoxicity Assay. First, the samples were sterilized with UV light for 4 h. The conditioned medium was prepared to understand any possible toxic effect induced by the possible ionic leach-out of the product from the samples into the medium. With this aim, 3 mL of the fresh medium was added to tubes with a certain mass of the tested material, which were kept in an incubator. After 72 h, the conditioned medium was collected and used in cytotoxicity tests. MTT assays of the film samples were performed in a 96-well plate. HFF-1 cells (about 1×10^5 cells per well) were seeded with a conditioned sample solution medium and incubated for 72 h. Following 72 h of incubation, a volume of 10 μL of 5 mg/mL MTT dye solution was added to each well. The cells were incubated at 37 °C for 3−4 h. MTT was taken up by active cells and reduced in the mitochondria to an insoluble purple formazan granule.[45] Cell viability was measured by determining mitochondrial NADH/NADPH-dependent dehydrogenase activity, which resulted in the cellular conversion of the 3-(4,5′-dimethylthiazol-2-yl)-5-(3-carboxymethoxylphenyl)-2-(4-sulfophenyl)-2*H*-tetrazolium salt into a soluble formazan dye. Subsequently, the supernatant was discarded, the precipitated formazan was dissolved in dimethyl sulfoxide (100 μL per well), and the optical density of the solution was evaluated using a Rayto Microplate Reader (RT-2100C, Shenzhen, China) at a wavelength of 570 nm. The statistical analysis was performed using GraphPad Prism statistical software (GraphPad Prism, version 10.0.1).

2.8. Antibacterial Activity Test. The standard strains Gram-positive bacteria *S. aureus* (ATCC 6538) and Gram-negative bacteria *E. coli* (ATCC 8739) were used to investigate the antibacterial activity of Ca-Alg, 0.5-Ca-Alg, 0.5-Ca-Alg-1/AgNW, and 0.5-Ca-Alg-3/AgNW films according to the ISO 22196, 2011. Following 24 h of incubation at 37 °C, the bacterial growth was examined by the colony forming unit (CFU) method to determine the count of the bacteria.

2.9. Water Vapor Permeability Test. The water vapor permeability (WVP) test of the Ca-Alg, 0.02-Ca-Alg, 0.1-Ca-Alg, 0.5-Ca-Alg, 0.5-Ca-Alg-1/AgNW, and 0.5-Ca-Alg-3/AgNW films, which were prepared from a total volume of 5 mL of the film solution following the procedure explained in Section 2.2, was performed following the standard method of ASTM E96/E96M-16 with some modifications. First, the glass laboratory test tubes were filled with 12 mL of distilled water, and then the film samples were stretched to the top sides of the tubes with plastic tapes. The total mass of the test tubes was weighed and recorded. The tubes were conditioned by a steady-state position at 23 ± 2 °C and 65 ± 5% humidity conditions for 8 h in the laboratory. Finally, the tubes were weighed at the testing time. The WVP test was repeated two times, and the water vapor transmission rate (WVTR) of the films was calculated from the equation below

$$\mathrm{WVTR}\left(\frac{g}{m^2 h}\right) = \frac{M_i - M_f}{AT} \quad (1)$$

where M_i and M_f are the initial and final masses of the tubes sealed with the samples, respectively, A is the area of the mouth of the test tube, and T is the time.

2.10. Swelling Experiments. To test the swelling ratio of the films, sample films were gently cut into 1.5 cm × 1.5 cm square shapes. The dry film pieces were soaked in 100 mL of distilled water and simulated body fluid (SBF) at 25 °C after the measurements of their initial mass values. SBF at pH = 7.4

https://doi.org/10.1021/acsomega.4c02467
ACS Omega 2024, 9, 49032−49042

was prepared by adding specific ion salts in 800 mL of distilled water, adjusting the pH of the solution with HCl and Tris, and finally diluting the final volume to 1 L.[46] The film pieces were taken out from the swelling media and then dried carefully with a paper towel to remove the excess liquid from the surface of the films. Then, the mass of the films was weighed on an analytical balance (KERN ABS 120-4N, Kern & Sohn GmbH, Balingen, Germany) at certain times (5, 15, 30, 45, and 60 min) of the steady-state gravimetric mass weighing experiment. The experiments were conducted in three parallel sets of experiments. The swelling ratio percentage of Ca-Alg and 0.5-Ca-Alg film samples was calculated using the equation below

$$\text{swelling ratio } \% = \frac{(m_i - m_f)}{m_i} \times 100 \quad (2)$$

where m_i and m_f are the film samples' initial and swelled masses in distilled water or SBF solution after a swelling time, respectively.

2.11. Transparency Analysis and Thickness of Films. To examine the transmittance properties of Ca-Alg-based films (Ca-Alg, 0.02-Ca-Alg, 0.1-Ca-Alg, and 0.5-Ca-Alg), the light transmittance in the ultraviolet−visible (UV−vis) light region was recorded by locating the film samples, which were cut in 2 cm × 3 cm dimensions, in a spectrophotometer. The transmittance spectra of the films were measured by a Shimadzu UV-2600i model spectrophotometer (Kyoto, Japan) at wavelengths between 200 and 800 nm. To calculate the opacity values of the Ca-Alg films, the transparency at a wavelength of 600 nm was used to calculate the opacity values of the films using the following equation

$$\text{opacity } (\text{mm}^{-1}) = -\frac{\log (T_{600})}{t} \quad (3)$$

where T_{600} is the transmittance at 600 nm and t is the average thickness of the film (mm).

A Mitutoyo digital caliper (Mitutoyo Corporation, Kanagawa, Japan) with 0.001 mm sensitivity was used to determine the thickness of the films at seven random points on each whole film, which was represented as the mean value with its standard deviation.

2.12. Statistical Analysis. The statistical analysis was performed using MINITAB Version 16.0 (MINITAB, State College, Pennsylvania). The one-way analysis of variance (ANOVA) and Tukey's multiple comparison test with a confidence level of 95% ($p < 0.05$) were used to investigate the significant differences.

3. RESULTS AND DISCUSSION

3.1. Characterization of Films. In order to investigate the effect of the amount of PVA on the creation of pores in the film structure, the concentration of PVA in Na-Alg films was varied as 0.02%, 0.1%, and 0.5% (w/v), while the other parameters in the film preparation step were kept constant. The digital photographs of Ca-Alg, 0.02-Ca-Alg, 0.1-Ca-Alg, and 0.5-Ca-Alg are given in Figure 1a−d. It is known that the opacity is affected by the physical characteristics of materials and correlated to the scattering of visible light. It is seen from Figure 1 that Ca-Alg and 0.02-Ca-Alg films have higher transparency, while 0.1-Ca-Alg and 0.5-Ca-Alg films have more opacity under visible light. To confirm this situation with a spectroscopic measurement, the light transmittance percentages of the films under UV−vis light were measured. The light

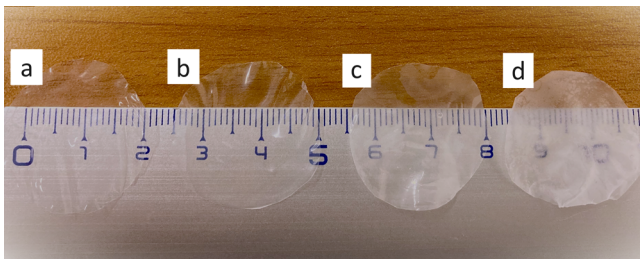

Figure 1. Digital photographs of Ca-Alg (a), 0.02-Ca-Alg (b), 0.1-Ca-Alg (c), and 0.5-Ca-Alg (d) films.

transmittance spectra of Ca-Alg films, which are shown in Figure 1, are given in Figure 2. The opacity of the films was

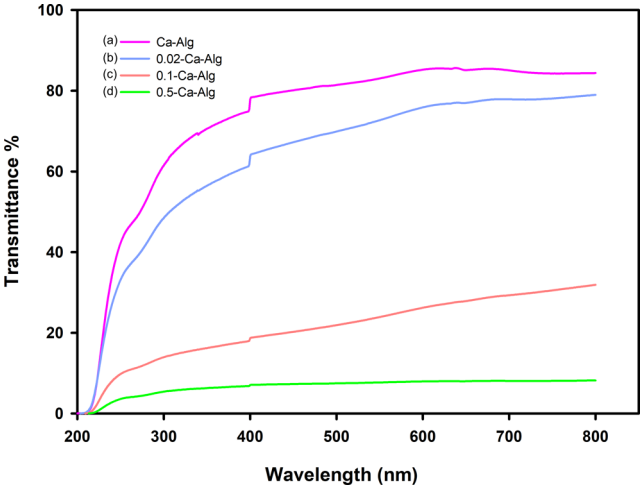

Figure 2. Transmittance percentage versus wavelength curves of Ca-Alg (a), 0.02-Ca-Alg (b), 0.1-Ca-Alg (c), and 0.5-Ca-Alg (d) films.

calculated using the thickness of the films and absorbance values at 600 nm obtained from transmittance spectra. Table 2

Table 2. Opacity and Thickness Values of the Ca-Alg Films[a]

film sample	opacity (mm^{-1})	thickness (mm)
Ca-Alg	0.35 ± 0.002^{B}	0.20 ± 0.01^{B}
0.02-Ca-Alg	0.59 ± 0.021^{C}	0.21 ± 0.01^{AB}
0.1-Ca-Alg	2.67 ± 0.041^{B}	0.22 ± 0.00^{A}
0.5-Ca-Alg	4.79 ± 0.011^{A}	0.23 ± 0.01^{A}

[a]Mean values with different superscripts indicate significant differences ($p < 0.05$) among the samples within the same column, according to Tukey's test.

represents the opacity values of Ca-Alg films. It is seen that the opacity of the films has been varied significantly ($p < 0.05$). As a result, it was seen that the light transmittance of Ca-Alg films decreased, as they had a porous structure. Porous Ca-Alg films have been recommended for wound care because they have low light transmittance and can protect the wound from UV light.

As shown in Figures 3 and S2, increasing the PVA content in the Na-Alg film results in larger pores after removing the water-soluble PVA in the cross-linked Ca-Alg films. Larger pores significantly create rough surfaces and scatter the visible light, resulting in less transparent Ca-Alg films. The pore sizes of the films were counted by using ImageJ. The pores were chosen randomly from 20 places on the film surface, and the calculated

https://doi.org/10.1021/acsomega.4c02467
ACS Omega 2024, 9, 49032−49042

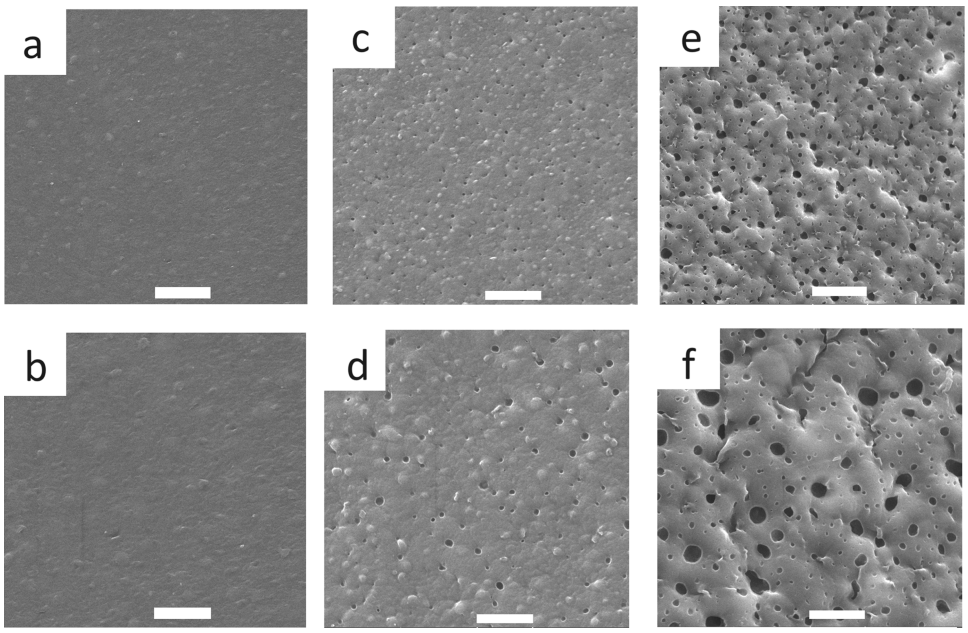

Figure 3. SEM micrographs of 0.02-Ca-Alg (a, b), 0.1-Ca-Alg (c, d), and 0.5-Ca-Alg (e, f) films. Scale bars are 2500× for 10 μm (a, c, e) and 5000× for 5 μm (b, d, f).

pore diameters are shown in Figure 4. While 0.02-Ca-Alg has a pore size of 0.6 ± 0.1 μm, increasing the PVA concentration to

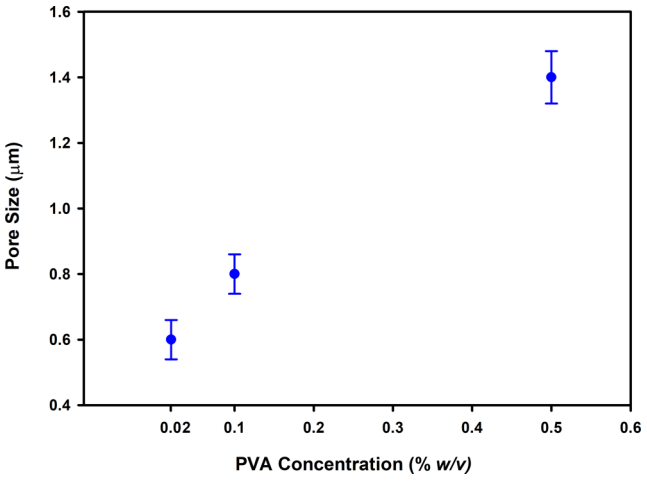

Figure 4. Pore size of the Ca-Alg films as a function of PVA concentration.

0.1% (w/v) in the Na-Alg film solution results in slightly larger pores with an average pore diameter of 0.8 ± 0.1 μm. 0.5-Ca-Alg films have the largest pores, with an average pore diameter of 1.4 ± 0.1 μm (see Figures 3 and 4). On the other hand, when the amount of PVA in the film is more than 0.5% (w/v) in the Na-Alg film solution, it is understood from the spectra taken by FTIR spectroscopy that PVA remains in the film and is not fully separated from the Ca-Alg film structure during the cross-linking and washing stages. The FTIR spectra are shown in Figure S3. In the PVA spectrum, the asymmetrical CH_2 stretching vibrations appear at 2938 cm^{-1}, and this peak is clearly seen in the 2-Ca-Alg spectra. The SEM image of the 2-Ca-Alg film is given in Figure S4. As can be seen from Figure S4, a PVA amount of more than 0.5% (w/v) in the Na-Alg solution prevents the formation of Ca-Alg films with uniform gaps, and this amount is considered the optimal concentration for the initial amount of PVA in the Na-Alg film solution. It has been found that PVA granules may block the pores of Ca-Alg films, and the ideal porous structure cannot be reached even at higher PVA amounts of more than 0.5% in the initial Na-Alg film solution.

3.2. Cell Adhesion Tests and AgNW Coating. To investigate the potential of the porous Ca-Alg-based films as a wound dressing material, the biocompatibility of the films was analyzed with cell proliferation studies using human foreskin fibroblast cells. The HFF-1 cells were seeded on Ca-Alg, 0.02-Ca-Alg, 0.1-Ca-Alg, and 0.5-Ca-Alg films for 5 days. After 5 days of incubation, SEM images of the samples were taken and are shown in Figures 5a–d and S5a–d. From Figure 5, it can be seen that no cell attachment occurs on the films except for the porous 0.5-Ca-Alg film. In Figure 5d, one of the attached cells is colored and highlighted by showing it within a square frame. Since cells did not adhere to Ca-Alg, 0.02-Ca-Alg, and 0.1-Ca-Alg films, it was concluded that pore size in the 0.5-Ca-Alg films was more suitable for cell proliferation. Thus, 1 and 3 wt % AgNWs were coated on the 0.5-Ca-Alg films, and further experiments were conducted on the AgNW-coated and not-coated porous 0.5-Ca-Alg films.

The 0.5-Ca-Alg films and 1 and 3 wt % AgNW-coated versions of these films were examined for cell adhesion ability to test the biocompatibility of the materials. As clearly shown in Figures 6a–c and S6a–c, cells can attach not only to 0.5-Ca-Alg films but also to 1 and 3 wt % AgNW-coated films. In addition, SEM images at lower magnifications (see Figures 6d–f and S6d–f) reveal a higher number of HFF-1 cells attached to the AgNW-coated films. The area fractions of the total area where the cells are located, as shown in Figure 6e,f, for the entire image are found to be 27 and 38% using the ImageJ program. Here, it was observed that by increasing the amount of AgNWs coated on the 0.5-Ca-Alg film from 1 to 3%, the cell adhesion property of the porous film also increased. Therefore, it was concluded that AgNW coating further enhanced the cell attachment to the porous 0.5-Ca-Alg

https://doi.org/10.1021/acsomega.4c02467
ACS Omega 2024, 9, 49032−49042

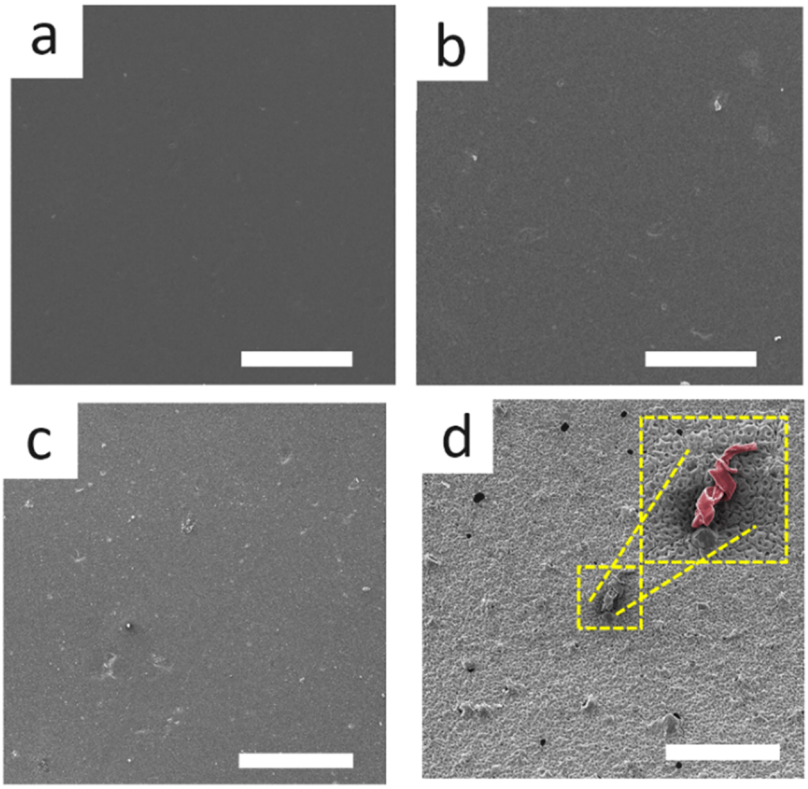

Figure 5. SEM images of Ca-Alg (a), 0.02-Ca-Alg (b), 0.1-Ca-Alg (c), and 0.5-Ca-Alg (d) films after the cell adhesion experiments (magnification is 200×, and the scale bar is 200 μm in (a−d)).

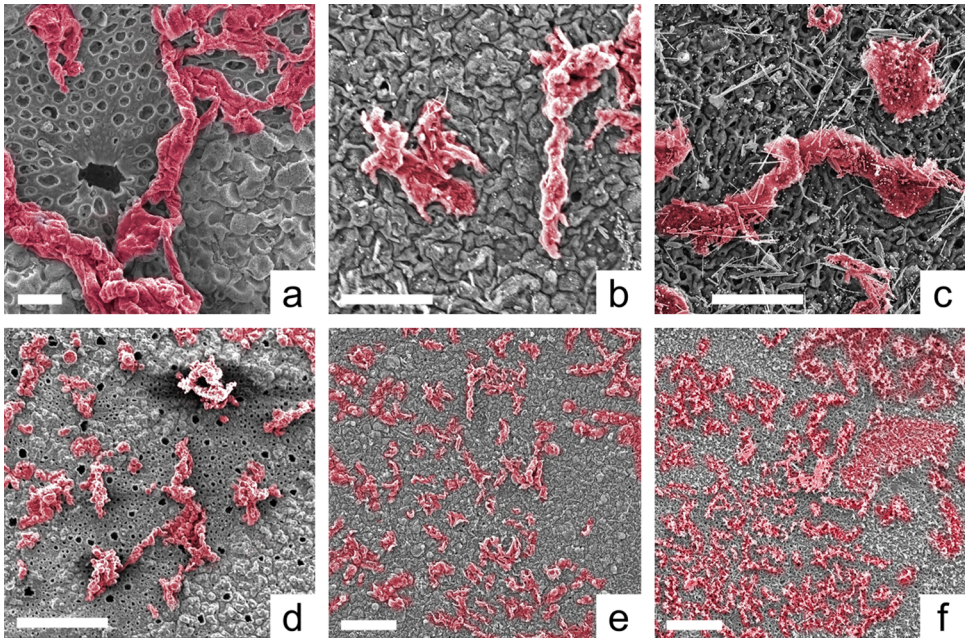

Figure 6. SEM images of HFF-1 cell attachment on 0.5-Ca-Alg (a, d), 0.5-Ca-Alg-1/AgNW (b, e), and 0.5-Ca-Alg-3/AgNW (c, f) films (magnification is 1000× for a scale bar of 20 μm (a), 2000× for a scale bar of 20 μm (b, c), 200× for a scale bar of 200 μm (d), and 500× for a scale bar of 50 μm (e, f)).

films. After the cell adhesion experiments, deterioration of the surface features of the 0.5-Ca-Alg films was observed (see Figures S7a−c and S8a−c), which did not affect the cell adhesion characteristics in a negative manner.

3.3. Cell Culture of the Films. The MTT assay is a generally suggested cytotoxicity test for the biocompatibility evaluation of biodegradable materials. Bagadoran et al. investigated the cell viability of the PVA/sodium alginate hydrogel scaffold with polycaprolactone microspheres proposed for wound healing against L929 cells for 1 day, 3 days, and 5 days. They concluded that there was no significant difference in terms of cell viability between 3 and 5 days of an

https://doi.org/10.1021/acsomega.4c02467
ACS Omega 2024, 9, 49032−49042

assay, and sodium alginate-PVA-based scaffolds were non-cytotoxic.[47] In the present study, the cytotoxicity of 0.5-Ca-Alg samples and 1 and 3 wt % AgNW-coated 0.5-Ca-Alg samples was investigated using an indirect contact MTT assay, and the results are shown in Figure 7. The cell viability of HFF-1 cells

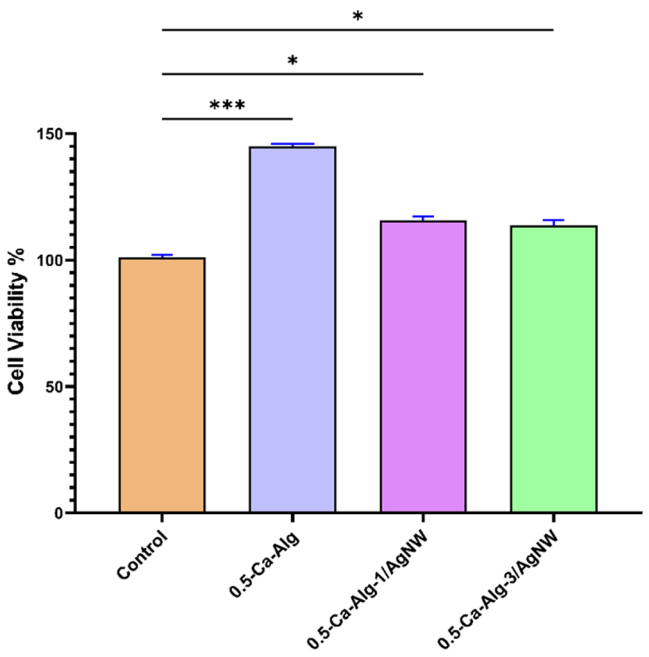

Figure 7. From left to right: the cell viability of HFF-1 cells through the MTT assay for control, 0.5-Ca-Alg, 0.5-Ca-Alg-1/AgNW, and 0.5-Ca-Alg-3/AgNW films at 72 h (Dunnett's multiple comparison test was performed; significant differences are represented by *p < 0.1 vs control and *** p < 0.001 vs control).

through the MTT assay for 0.02-Ca-Alg and 0.1-Ca-Alg is shown in Figure S9. The MTT assay was conducted by using HFF-1 cell lines during 72 h of exposure time. The cytotoxicity test indicated that all Ca-Alg samples had no cytotoxic effect compared to control (HFF-1) at 72 h. Moreover, the cell growth and viability on all of the porous Ca-Alg-based film samples increased after 72 h. As a result, the biocompatibility test demonstrated that all of the prepared Ca-Alg-based films had suitable cytocompatibility and could be utilized for the further development of biomedical applications.

3.4. Antibacterial Activity. The studies previously reported in the literature[48,49] emphasized that improving the antibacterial properties of natural polymers would make these materials usable in various applications, especially in wound care. Research on the antibacterial properties of polymeric materials that may be candidates for wound healing has also been conducted in different studies.[50,51] To prevent bacterial infection and fasten the wound healing process, the positive effect of silver and silver compounds has been investigated in several studies.[18,19,21,28,52] It is known that commercially available calcium alginate wound dressing materials with 1.4% silver (ALGICELL Ag) have antibacterial properties against *S. aureus* and *P. aeruginosa* bacteria.[53,54] The increasing antibacterial activity of the biopolymer-based materials after coating with AgNWs had been previously reported in other studies.[32−34] Hereby, AgNWs have been coated on alginate films for the first time. The antibacterial activities of nonporous (Ca-Alg), porous (0.5-Ca-Alg), and AgNW-coated porous (0.5-Ca-Alg-1/AgNW and 0.5-Ca-Alg-3/AgNW) films were evaluated against Gram-positive and Gram-negative bacteria, namely, *S. aureus* and *E. coli*, respectively. The number of both Gram-positive and Gram-negative bacteria increased after 24 h of incubation on the Ca-Alg and 0.5-Ca-Alg films (see Figure 8). Thus, neither nonporous nor porous Ca-Alg films exhibited the inhibition of bacterial growth. However, the addition of even 1 wt % AgNW onto the porous 0.5-Ca-Alg film significantly enhanced the antibacterial activity and resulted in a significant decrease in log CFU/mL values after 24 h. Therefore, AgNW coating not only resulted in higher cell proliferation but also provided a bactericidal property to the porous Ca-Alg films.

3.5. Water Vapor Permeability Test. The WVTR of a wound dressing plays a critical role in the wound healing process. The WVTR ability of the dressing directly affects the wound area in terms of water gain or water loss by moisture transition. Moreover, it is necessary in the wound healing process to keep the wound area under specified moisture conditions.[55] In this study, the WVTR values of Ca-Alg, 0.02-Ca-Alg, 0.1-Ca-Alg, 0.5-Ca-Alg, 0.5-Ca-Alg-1/AgNW, and 0.5-Ca-Alg-3/AgNW films are shown in Figure S10. The WVTR

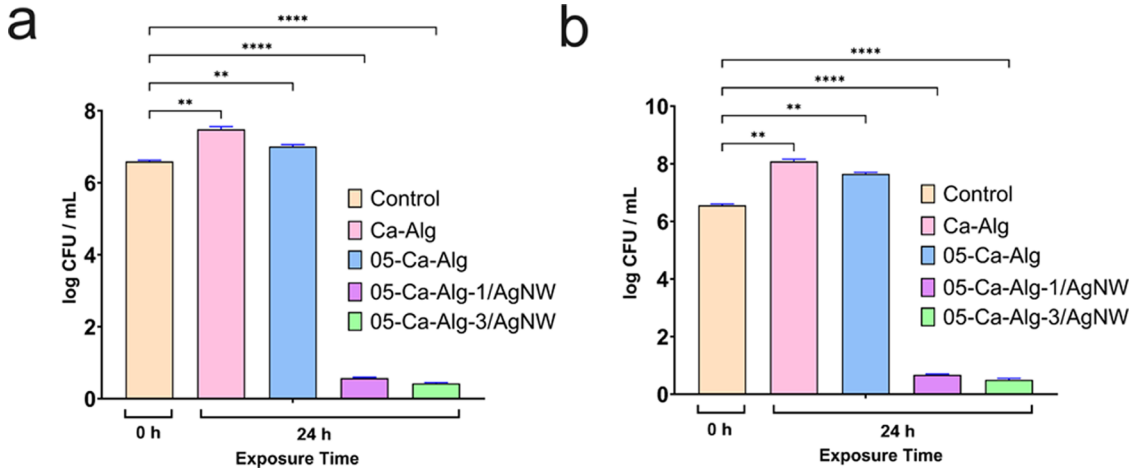

Figure 8. Bar graphs showing the organism count versus exposure time of *S. aureus* (a) and *E. coli* (b) (Dunnett's multiple comparison test was performed; significant differences are represented by **p < 0.01 vs control and **** p < 0.0001 vs control).

https://doi.org/10.1021/acsomega.4c02467
ACS Omega 2024, 9, 49032−49042

values of Ca-Alg-based films, Ca-Alg, 0.5-Ca-Alg, 0.5-Ca-Alg-1/Ca-Alg, and 0.5-Ca-Alg-3/Ca-Alg, were determined and are plotted in Figure 9. Table 3 shows the calculated WVTR (g/m^2 h) values of Ca-Alg, 0.5-Ca-Alg, 0.5-Ca-Alg-1/Ca-Alg, and 0.5-Ca-Alg-3/Ca-Alg samples. The passage of water molecules through the porous structure of the films has become more facile compared to nonporous films. The WVTR values of Ca-Alg and porous 0.5-Ca-Alg films were calculated as 62.51 ± 0.91 and 82.45 ± 1.23 g/m^2 h, respectively. Although pores on the 0.5-Ca-Alg films are in the micron scale, it has an ∼30% higher WVTR value than the nonporous Ca-Alg film. The WVTR values of the 1% and 3 wt % AgNW-coated porous films increased as well and were determined as 90.14 ± 2.03 and 110.2 ± 1.75 g/m^2 h, respectively. It was observed that there was an increase in the water vapor permeability rate of films coated with AgNWs. This indicates that after the nanowire coating process of the films, the physical properties of the films are improved thanks to AgNWs positively developing the permeability effect with their presence on the film surface. AgNWs adhering to the surface of the film had not closed the pores of the 0.5-Ca-Alg film and had not reduced the WVTR. On the contrary, it was shown that the existence of AgNWs on the film surface allowed good water vapor permeability and supported the hydrophilic structure of the film.

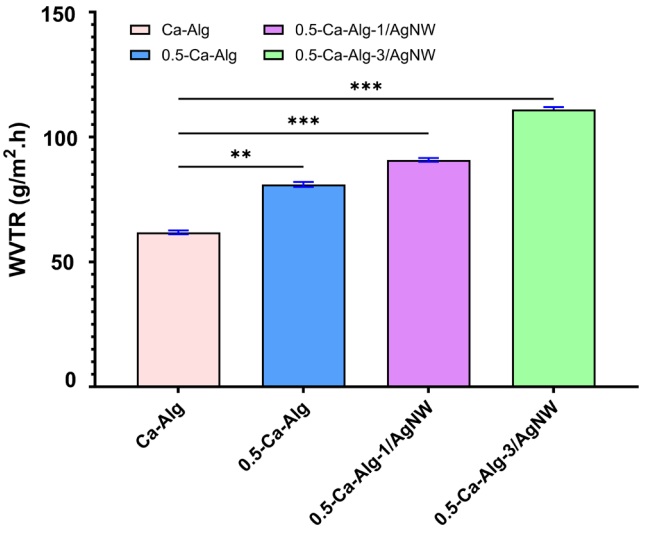

Figure 9. Bar graph showing the WVTR values of Ca-Alg, 0.5-Ca-Alg, 0.5-Ca-Alg-1/AgNW, and 0.5-Ca-Alg-3/AgNW films (Dunnett's multiple comparison test was performed; significant differences are represented by $^{**}p < 0.01$ vs control, and $^{***}p < 0.001$ vs control).

3.6. Swelling Test. Swelling experiments of Ca-Alg and 0.5-Ca-Alg films were performed to investigate the swelling ability of the films in distilled water and SBF (pH = 7.4). The swelling ratio percentage of the film samples was determined as a function of the change of the mass over time, and the results are given in Figure 10a,b. The swelling equilibrium of the films was reached at 60 min in distilled water and SBF. The swelling ratio percentages of Ca-Alg, 0.5-Ca-Alg, 0.5-Ca-Alg-1/AgNW, and 0.5-Ca-Alg-3/AgNW films are listed in Table 3 at an equilibrium swelling time of 60 min. The maximum swelling of the Ca-Alg film was 88.97 ± 8.02 and 162.42 ± 6.22%, while the porous 0.5-Ca-Alg film swelled 118.78 ± 4.59 and 226.60 ± 15.25% in distilled water and SBF, respectively. The swelling of Ca-Alg and 0.5-Ca-Alg films was ∼2 times enhanced in SBF compared to that in distilled water. The presence of the pores in the 0.5-Ca-Alg film, as shown in Figure 3e,f, provided an increase in both distilled water and SBF absorbencies of the films. This correlation is also consistent with the variation of the WVTR rates given in Section 3.5. AgNW-coated films have slightly higher swelling ratios compared to noncoated porous films. In a study performed by Wang et al., AgNWs were coated on a biopolymer gelatin film, and it was concluded that

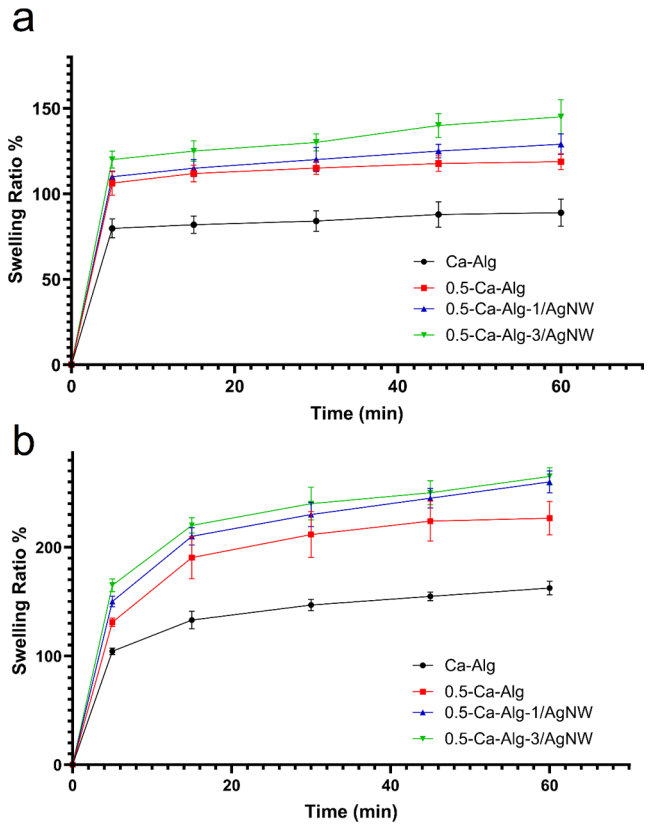

Figure 10. Swelling ratio (%) versus time (min) graphs of Ca-Alg, 0.5-Ca-Alg, 0.5-Ca-Alg-1/AgNW, and 0.5-Ca-Alg-3/AgNW films in distilled water (a) and in SBF (pH = 7.4) (b).

Table 3. WVTR and Swelling Ratio Percentages of the Ca-Alg Films[a]

film sample	WVTR (g/m^2 h)	swelling ratio % in distilled water at 60 min	swelling ratio % in SBF at 60 min
Ca-Alg	62.51 ± 0.91^{A}	88.97 ± 8.02^{C}	162.42 ± 6.22^{C}
0.5-Ca-Alg	82.45 ± 1.23^{B}	118.78 ± 4.59^{B}	226.60 ± 15.25^{B}
0.5-Ca-Alg-1/AgNW	90.14 ± 2.03^{C}	129.00 ± 6.01^{AB}	260.05 ± 10.1^{A}
0.5-Ca-Alg-3/AgNW	110.2 ± 1.75^{D}	145.20 ± 10.01^{A}	265.20 ± 8.00^{A}

[a]Mean values with different superscripts indicate significant differences ($p < 0.05$) among the samples within the same column, according to Tukey's test.

https://doi.org/10.1021/acsomega.4c02467
ACS Omega 2024, 9, 49032−49042

AgNWs increased the swelling property of the material thanks to their adhesion behavior and hydrogen bonds to the biopolymer.[56] Similarly, the AgNW-coated porous Ca-Alg film exhibited an enhanced swelling ratio after the coating with AgNWs. This showed that, thanks to the adhesion of AgNWs to the film, the film could exhibit improved swelling ability even in an aqueous environment. Porous Ca-Alg films with water absorption properties are recommended as functional wound care materials for the care of wounds that may have wound fluids.

4. CONCLUSIONS

In this study, porous Ca-Alg films were prepared via the removal of PVA during the cross-linking process. It is demonstrated that the amount of PVA in the Na-Alg solution affects the generated pore size on the Ca-Alg films. Cell attachment experiments conducted on the nonporous Ca-Alg film and Ca-Alg films with three different pore sizes indicate that HFF-1 cells only adhere to the 0.5-Ca-Alg films that have an average pore size of 1.4 μm. The 0.5-Ca-Alg films were further coated with 1 and 3 wt % AgNWs to improve the antibacterial activity of the AgNWs. All of the AgNW-coated samples exhibit an excellent bactericidal effect against *S. aureus* and *E. coli* bacteria. In addition, coated porous films were not cytotoxic against fibroblast cells, and cell proliferation on the AgNW-coated porous samples was enhanced. Both 1% and 3 wt % AgNW-coated 0.5-Ca-Alg films exhibit superior water vapor permeability and swelling ratios in water and SBF. These aforementioned properties make the AgNW-coated porous 0.5-Ca-Alg films an ideal candidate for active wound dressing applications.

■ ASSOCIATED CONTENT

Supporting Information

The Supporting Information is available free of charge at https://pubs.acs.org/doi/10.1021/acsomega.4c02467.

Original scaled bar versions of the scanning electron microscopy images of Ca-Alg films; FTIR spectroscopy analysis; and detailed information about cell viability and WVTR tests (PDF)

■ AUTHOR INFORMATION

Corresponding Author

Alper Güraslan − *Faculty of Textile Technologies and Design, Department of Textile Engineering, Istanbul Technical University, Istanbul 34437, Turkey;* orcid.org/0000-0001-7641-4611; Phone: 90-212-251 88 08; Email: guraslan@itu.edu.tr; Fax: 90-212-251 88 29

Authors

Nilay Kahya − *Faculty of Science and Letters, Department of Chemistry, Istanbul Technical University, Istanbul 34469, Turkey;* orcid.org/0000-0002-7884-5113

Aslin Kartun − *Faculty of Textile Technologies and Design, Department of Textile Engineering, Istanbul Technical University, Istanbul 34437, Turkey;* orcid.org/0009-0003-8151-9911

Işık Neslişah Korkut − *Faculty of Medicine, Department of Physiology, Istanbul University, Istanbul 34093, Turkey;* orcid.org/0000-0001-8550-5400

Canan Usta − *Faculty of Textile Technologies and Design, Department of Textile Engineering, Istanbul Technical University, Istanbul 34437, Turkey;* orcid.org/0000-0002-9489-8768

Dürdane Serap Kuruca − *Faculty of Medicine, Department of Physiology, Istanbul Atlas University, Istanbul 34408, Turkey*

Complete contact information is available at: https://pubs.acs.org/10.1021/acsomega.4c02467

Notes

The authors declare no competing financial interest.

■ ACKNOWLEDGMENTS

This study is supported within the scope of the Scientific and Technological Research Council of Turkey (TUBITAK) 3501-Career Development Program (CAREER; Grant No. 221M272) and is also supported by TUBITAK BIDEB 2209-A University Students Research Projects Support Program with the application number 1919B012205882.

■ REFERENCES

(1) Kim, S.; Baek, S.; Sluyter, R.; Konstantinov, K.; Kim, J. H.; Kim, S.; Kim, Y. H. Wearable and implantable bioelectronics as eco-friendly and patient-friendly integrated nanoarchitectonics for next-generation smart healthcare technology. *EcoMat* **2023**, *5* (8), No. e12356.

(2) Jiang, W.; Zhang, X.; Liu, P.; Zhang, Y.; Song, W.; Yu, D. G.; Lu, X. Electrospun healthcare nanofibers from medicinal liquor of *Phellinus igniarius*. *Adv. Compos. Hybrid Mater.* **2022**, *5* (4), 3045−3056.

(3) Lu, S.; Wu, H.; Ge, S.; Huang, L.; Chen, L.; Connor, C.; Guo, Z.; Jiang, Y.; Xu, B. B.; Peng, W. A cellulose/chitosan dual-crosslinked multifunctional and resilient hydrogel for emergent open wound management. *Adv. Healthcare Mater.* **2024**, No. 2304676.

(4) Kuddushi, M.; Deng, X.; Nayak, J.; Zhu, S.; Xu, B. B.; Zhang, X. A transparent, tough and self-healable biopolymeric composites hydrogel for open wound management. *ACS Appl. Bio Mater.* **2023**, *6* (9), 3810−3822.

(5) Azarian, M. H.; Junyusen, T.; Sutapun, W. Biogenic vaterite calcium carbonate-silver/poly(vinyl alcohol) film for wound dressing. *ACS Omega* **2024**, *9* (1), 955−969.

(6) Laurano, R.; Boffito, M.; Ciardelli, G.; Chiono, V. Wound dressing products: a translational investigation from the bench to the market. *Eng. Regener.* **2022**, *3* (2), 182−200.

(7) Kaya, S.; Derman, S. Properties of ideal wound dressing. *J. Fac. Pharm. Ankara Univ.* **2023**, *47* (3), 1119−1131.

(8) Rezvani Ghomi, E.; Khalili, S.; Khorasani, S. N.; Neisiany, R. E.; Ramakrishna, S. Wound dressings: current advances and future directions. *J. Appl. Polym. Sci.* **2019**, *136* (27), 47738.

(9) Vivcharenko, V.; Trzaskowska, M.; Przekora, A. Wound dressing modifications for accelerated healing of infected wounds. *Int. J. Mol. Sci.* **2023**, *24* (8), 7193.

(10) Liang, Y.; Liang, Y.; Zhang, H.; Guo, B. Antibacterial biomaterials for skin wound dressing. *Asian J. Pharm. Sci.* **2022**, *17* (3), 353−384.

(11) Parham, S.; Kharazi, A. Z.; Bakhsheshi-Rad, H. R.; Kharaziha, M.; Ismail, A. F.; Sharif, S.; Razzaghi, M.; RamaKrishna, S.; Berto, F. Antimicrobial synthetic and natural polymeric nanofibers as wound dressing: a review. *Adv. Eng. Mater.* **2022**, *24* (6), No. 2101460.

(12) Alexander, J. W. History of the medical use of silver. *Surg. Infect.* **2009**, *10* (3), 289−292.

(13) Medici, S.; Peana, M.; Nurchi, V. M.; Zoroddu, M. A. Medical uses of silver: history, myths, and scientific evidence. *J. Med. Chem.* **2019**, *62* (13), 5923−5943.

(14) Politano, A. D.; Campbell, K. T.; Rosenberger, L. H.; Sawyer, R. G. Use of silver in the prevention and treatment of infections: silver review. *Surg. Infect.* **2013**, *14* (1), 8−20.

(15) Konop, M.; Damps, T.; Misicka, A.; Rudnicka, L. Certain aspects of silver and silver nanoparticles in wound care: a minireview. *J. Nanomater.* **2016**, *2016*, No. 7614753.

(16) Nqakala, Z. B.; Sibuyi, N. R. S.; Fadaka, A. O.; Meyer, M.; Onani, M. O.; Madiehe, A. M. Advances in nanotechnology towards development of silver nanoparticle-based wound-healing agents. *Int. J. Mol. Sci.* **2021**, *22* (20), 11272.
(17) Boroumand, Z.; Golmakani, N.; Boroumand, S. Clinical trials on silver nanoparticles for wound healing. *Nanomed. J.* **2018**, *5* (4), 186−191.
(18) Moore, C.; Young, J. Effectiveness of silver in wound care treatment. *Phys. Ther. Rev.* **2011**, *16* (3), 201−209.
(19) Rodriguez-Arguello, J.; Lienhard, K.; Patel, P.; Geransar, R.; Somayaji, R.; Parsons, L.; Conly, J.; Ho, C. A scoping review of the use of silver-impregnated dressings for the treatment of chronic wounds. *Ostomy Wound Manage* **2018**, *64* (3), 14−31.
(20) Rai, M.; Yadav, A.; Gade, A. Silver nanoparticles as a new generation of antimicrobials. *Biotechnol. Adv.* **2009**, *27* (1), 76−83.
(21) Kalwar, K.; Shan, D. Antimicrobial effect of silver nanoparticles (AgNPs) and their mechanism − a mini review. *Micro Nano Lett.* **2018**, *13* (3), 277−280.
(22) Anees Ahmad, S.; Das, S. S.; Khatoon, A.; Ansari, M. T.; Afzal, M.; Hasnain, M. S.; Nayak, A. K. Bactericidal activity of silver nanoparticles: a mechanistic review. *Mater. Sci. Energy Technol.* **2020**, *3*, 756−769.
(23) Bruna, T.; Maldonado-Bravo, F.; Jara, P.; Caro, N. Silver nanoparticles and their antibacterial applications. *Int. J. Mol. Sci.* **2021**, *22* (13), 7202.
(24) Baukum, J.; Pranjan, J.; Kaolaor, A.; Chuysinuan, P.; Suwantong, O.; Supaphol, P. The potential use of cross-linked alginate/gelatin hydrogels containing silver nanoparticles for wound dressing applications. *Polym. Bull.* **2020**, *77*, 2679−2695.
(25) Diniz, F. R.; Maia, R. C. A. P.; de Andrade, L. R. M.; Andrade, L. N.; Chaud, M. V.; da Silva, C. F.; Corrêa, C. B.; de Albuquerque Junior, R. L.; da Costa, L. P.; Shin, S. R.; Hassan, S.; Sanchez-Lopez, E.; Souto, E. B.; Severino, P. Silver nanoparticles-composing alginate/gelatine hydrogel improves wound healing in vivo. *Nanomaterials* **2020**, *10* (2), 390.
(26) Gurarslan, A.; Özdemir, B.; Bayat, İ. H.; Yelten, M. B.; Kurt, G. K. Silver nanowire coated knitted wool fabrics for wearable electronic applications. *J. Eng. Fibers Fabr.* **2019**, *14*, 1558925019856222 DOI: 10.1177/1558925019856222.
(27) Gurarslan, A. Wireless controlling of a toy robot using silver nanowire coated Spandex yarns. *J. Ind. Text.* **2019**, *49* (1), 46−57.
(28) Jones, R. S.; Draheim, R. R.; Roldo, M. Silver nanowires: Synthesis, antibacterial activity and biomedical applications. *Appl. Sci.* **2018**, *8* (5), 673.
(29) Zhang, P.; Wyman, I.; Hu, J.; Lin, S.; Zhong, Z.; Tu, Y.; Huang, Z.; Wei, Y. Silver nanowires: Synthesis Technologies, growth mechanism and multifunctional applications. *Mater. Sci. Eng.: B* **2017**, *223*, 1−23.
(30) Ha, H.; Amicucci, C.; Matteini, P.; Hwang, B. Mini Review of synthesis strategies of silver nanowires and their applications. *Colloid Interface Sci. Commun.* **2022**, *50*, No. 100663.
(31) Kim, J.-H.; Ma, J.; Jo, S.; Lee, S.; Kim, C. S. Enhancement of antibacterial properties of a silver nanowire film via electron beam irradiation. *ACS Appl. Bio Mater.* **2020**, *3* (4), 2117−2124.
(32) Li, J.; Li, L.; Lv, J.; Wang, C.; Liu, Y. Preparation of thiolated chitosan/silver nanowire composite hydrogels with antimicrobial activity for obstetric wound care. *Mater. Lett.* **2020**, *280*, No. 128497.
(33) Wan, Y.; Yang, S.; Wang, J.; Gan, D.; Gama, M.; Yang, Z.; Zhu, Y.; Yao, F.; Luo, H. Scalable synthesis of robust and stretchable composite wound dressings by dispersing silver nanowires in continuous bacterial cellulose. *Composites, Part B* **2020**, *199*, No. 108259.
(34) Zhao, Y.; Lu, Q.; Wu, J.; Zhang, Y.; Guo, J.; Yu, J.; Shu, X.; Chen, Q. Flexible, robust and self-peeling PLA/AgNWs nanofiber membranes with photothermally antibacterial properties for wound dressing. *Appl. Surf. Sci.* **2023**, *615*, No. 156284.
(35) Saraiva, M. M.; da Silva Campelo, M.; Câmara Neto, J. F.; Lima, A. B. N.; de Almeida Silva, G.; de Freitas Figueredo Dias, A. T.; Ricardo, N. M. P. S.; Kaplan, D. L.; Riberiro, M. E. N. P. Alginate/polyvinyl alcohol films for wound healing: advantages and challenges. *J. Biomed. Mater. Res., Part B* **2023**, *111* (1), 220−233.
(36) Tang, N. F. R.; Heryanto, H.; Armynah, B.; Tahir, D. Bibliometric analysis of the use of calcium alginate for wound dressing applications: a review. *Int. J. Biol. Macromol.* **2023**, *228*, 138−152.
(37) Zhang, M.; Zhao, X. Alginate hydrogel dressings for advanced wound management. *Int. J. Biol. Macromol.* **2020**, *162*, 1414−1428.
(38) Varaprasad, K.; Jayaramudu, T.; Kanikireddy, V.; Toro, C.; Sadiku, E. R. Alginate-based composite materials for wound dressing application: a mini review. *Carbohydr. Polym.* **2020**, *236*, No. 116025.
(39) Aderibigbe, B.; Buyana, B. Alginate in wound dressings. *Pharmaceutics* **2018**, *10* (2), 42.
(40) Hodge, J. G.; Zamierowski, D. S.; Robinson, J. L.; Mellott, A. J. Evaluating polymeric biomaterials to improve next generation wound dressing design. *Biomater. Res.* **2022**, *26* (1), 50.
(41) Sheokand, B.; Vats, M.; Kumar, A.; Srivastava, C. M.; Bahadur, I.; Pathak, S. R. Natural polymers used in the dressing materials for wound healing: past, present and future. *J. Polym. Sci.* **2023**, *61* (14), 1389−1414.
(42) Li, J.; Wu, Y.; He, J.; Huang, Y. A new insight to the effect of calcium concentration on gelation process and physical properties of alginate films. *J. Mater. Sci.* **2016**, *51* (12), 5791−5801.
(43) Jin, S. G. Production and application of Biomaterials based on Polyvinyl Alcohol (PVA) as wound dressing. *Chem. - Asian J.* **2022**, *17* (21), No. e202200595.
(44) Hu, G.; Varamesh, A.; Zhong, N.; Kong, F.; Hu, J. Super-strong and high-performance electrical film heater derived from silver nanowire/aligned bacterial cellulose film. *Bioresour Bioprocess.* **2023**, *10* (1), 54.
(45) Mosmann, T. Rapid colorimetric assay for cellular growth and survival: Application to proliferation and cytotoxicity assays. *J. Immunol. Methods* **1983**, *65* (1−2), 55−63.
(46) Marques, M. R. C.; Loebenberg, R.; Almukainzi, M. Simulated biological fluids with possible application in dissolution testing. *Dissolution Technol.* **2011**, *18* (3), 15−28.
(47) Bahadoran, M.; Shamloo, A.; Nokoorani, Y. D. Development of a polyvinyl alcohol/sodium alginate hydrogel-based scaffold incorporating BFGF-encapsulated microspheres for accelerated wound healing. *Sci. Rep.* **2020**, *10* (1), No. 7342.
(48) Dang, X.; Yu, Z.; Wang, X.; Li, N. Eco-friendly cellulose-based nonionic antimicrobial polymers with excellent biocompatibility, nonleachability, and polymer miscibility. *ACS Appl. Mater. Interfaces* **2023**, *15* (43), 50344−50359.
(49) Yan, L.; Dang, X.; Yang, M.; Han, W.; Li, Y. Novel hyperbranched dialdehyde carboxymethyl cellulose-grafted gelatin films as potential natural antibacterial materials. *ACS Sustainable Chem. Eng.* **2023**, *11* (19), 7323−7333.
(50) Yang, M.; Zhang, M.; Wang, Y.; Li, Y.; Han, W.; Dang, X. Silver nanoparticle-loaded gelatin-based nanocomposite films toward enhanced mechanical properties and antibacterial activity. *ACS Appl. Bio Mater.* **2022**, *5* (5), 2193−2201.
(51) Zhang, M.; Yang, M.; Woo, M. W.; Li, Y.; Han, W.; Dang, X. High-mechanical strength carboxymethyl chitosan-based hydrogel film for antibacterial wound dressing. *Carbohydr. Polym.* **2021**, *256*, No. 117590.
(52) Qin, Y. Silver-containing alginate fibres and dressings. *Int. Wound J.* **2005**, *2* (2), 172−176.
(53) ALGICELL Ag Antimicrobial Alginate Dressing. https://www.woundsource.com/product/algicell-ag-antimicrobial-alginate-dressing. (accessed Dec 3, 2023).
(54) ALGICELL-AG-IFU-Calcium Alginate Dressing with Antimicrobial Silver, Instructions for Use (USA). https://www.kromh.com/wp-content/uploads/ALGICELL-AG-IFU.pdf. (accessed Dec 3, 2023).
(55) Nuutila, K.; Eriksson, E. Moist wound healing with commonly available dressings. *Adv. Wound Care* **2021**, *10* (12), 685−698.
(56) Wang, G.; Hao, L.; Zhang, X.; Tan, S.; Zhou, M.; Gu, W.; Ji, G. Flexible and transparent silver nanowires/biopolymer film for high-

https://doi.org/10.1021/acsomega.4c02467
ACS Omega 2024, 9, 49032−49042

efficient electromagnetic interference shielding. *J. Colloid Interface Sci.* **2022**, *607*, 89−99.

https://doi.org/10.1021/acsomega.4c02467
ACS Omega 2024, 9, 49032−49042